Radiation-modified structure of $Ge_{25}Sb_{15}S_{60}$ and $Ge_{35}Sb_5S_{60}$ glasses

T. Kavetskyy,[1,2,3,a] O. Shpotyuk,[1,3] I. Kaban,[2] and W. Hoyer[2]
[1]*Institute of Materials, Scientific Research Company "Carat," 202 Stryjska Str., Lviv 79031, Ukraine*
[2]*Institute of Physics, Chemnitz University of Technology, D-09107 Chemnitz, Germany*
[3]*Institute of Physics, Jan Dlugosz University of Czestochowa, Al. Armii Krajowej 13/15, Czestochowa 42201, Poland*

(Received 8 February 2008; accepted 22 May 2008; published online 27 June 2008)

Atomic structures of $Ge_{25}Sb_{15}S_{60}$ and $Ge_{35}Sb_5S_{60}$ glasses are investigated in the γ-irradiated and annealed after γ-irradiation states by means of high-energy synchrotron x-ray diffraction technique. The first sharp diffraction peak (FSDP) is detected at around 1.1 $Å^{-1}$ in the structure factors of both alloys studied. The FSDP position is found to be stable for radiation/annealing treatment of the samples, while the FSDP intensity shows some changes between γ-irradiated and annealed states. The peaks in the pair distribution functions observed between 2 and 4 Å are related to the Ge–S, Ge–Sb, and Sb–Sb first neighbor correlations and Ge–Ge second neighbor correlations in the edge-shared $GeS_{4/2}$ tetrahedra, and S–S and/or Ge–Ge second neighbor correlations in the corner-shared $GeS_{4/2}$ tetrahedra. Three mechanisms of the radiation-/annealing-induced changes are discussed in the framework of coordination topological defect formation and bond-free solid angle concepts. © *2008 American Institute of Physics*. [DOI: 10.1063/1.2945300]

I. INTRODUCTION

Chalcogenide glasses are known as important optoelectronic materials intensively used in new generation infrared optical and memory devices.[1–4] Ge–As(Sb)–S(Se,Te) ternary systems are especially attractive due to (i) the possibility of wide variation of chemical compositions within glass forming region, (ii) anomalous compositional dependences of physical and chemical properties of glasses, (iii) photo- and radiation-induced phenomena, etc.[5–8]

In order to prepare glasses with optimal exploitation properties, various methods of chemical-technological modification have scrupulously been developed and improved by well-known world-wide industrial electronic companies. However, possibilities for chemical-technological modification are fully exhausted, in fact. Moreover, this does not correspond to the main principles of the modern human society—*energy saving and environment protection*—because of very expensive procedures such as multistate distillation, homogenized vacuum melting, vapor filtration, thermal decomposition, dissociate evaporation, melt centrifugation, fractioning, etc. Therefore, development of alternative energy-conserved and ecologically save methods of post-technological modification of chalcogenide glasses is a topical problem. Structural modification of the glass matrix by a high-energy γ-irradiation is one of the ways to resolve this problem. Principal advantages of γ-irradiation among other types of ionizing irradiation are discussed elsewhere.[9] A special attention in the radiation-modified materials should be paid to their new structural peculiarities attained after irradiation.

In the present work we investigate γ-irradiated and annealed afterward $Ge_{25}Sb_{15}S_{60}$ and $Ge_{35}Sb_5S_{60}$ glasses by means of high-energy synchrotron x-ray diffraction (XRD) technique. The aim is to study the atomic structure of the Ge–Sb–S glasses upon γ-irradiation and subsequent annealing and explore the possibilities of controlling/modifying the local atomic environment in the first and second coordination shells. Besides, a qualitative comparison of our annealed alloys and as-prepared $Ge_xSb_{40-x}S_{60}$ ($x=10$, 20, and 30) glasses studied recently by Kakinuma *et al.*[10] will be made. It has been shown in Ref. 11 that radiation-induced changes in optical properties of chalcogenide glasses are reversible with annealing at a temperature near glass transition T_g (10–20 K below it). It is interesting to see whether the atomic structure is reversible as well.

The structure of the article is organized as follows. In Sec. II we describe the sample preparation, irradiation, and thermal annealing procedures and provide some details of high-energy synchrotron XRD measurements and data treatment. In Sec. III, the experimental structure factors $S(Q)$ and corresponding pair distribution functions $g(r)$ are given and the main features of the first and second coordination shells are identified. Section IV presents analysis of the radiation-/annealing-induced changes in the pair distribution functions of $Ge_{25}Sb_{15}S_{60}$ and $Ge_{35}Sb_5S_{60}$ glasses related to the first and second coordination shells. Three different mechanisms responsible for the structural changes in $Ge_{25}Sb_{15}S_{60}$ and $Ge_{35}Sb_5S_{60}$ glasses upon γ-irradiation and consequent annealing are also discussed in this section. Final conclusions are summarized in Sec. V.

II. EXPERIMENTAL

$Ge_{25}Sb_{15}S_{60}$ and $Ge_{35}Sb_5S_{60}$ bulk glasses selected for the study were prepared from elements of 99.9999% purity in evacuated quartz ampoules by a melt quenching procedure,

[a]Author to whom correspondence should be addressed. Tel.: +38 (0322) 65-22-83. FAX: +38 (0322) 94-97-35. Electronic mail: kavetskyy@yahoo.com.

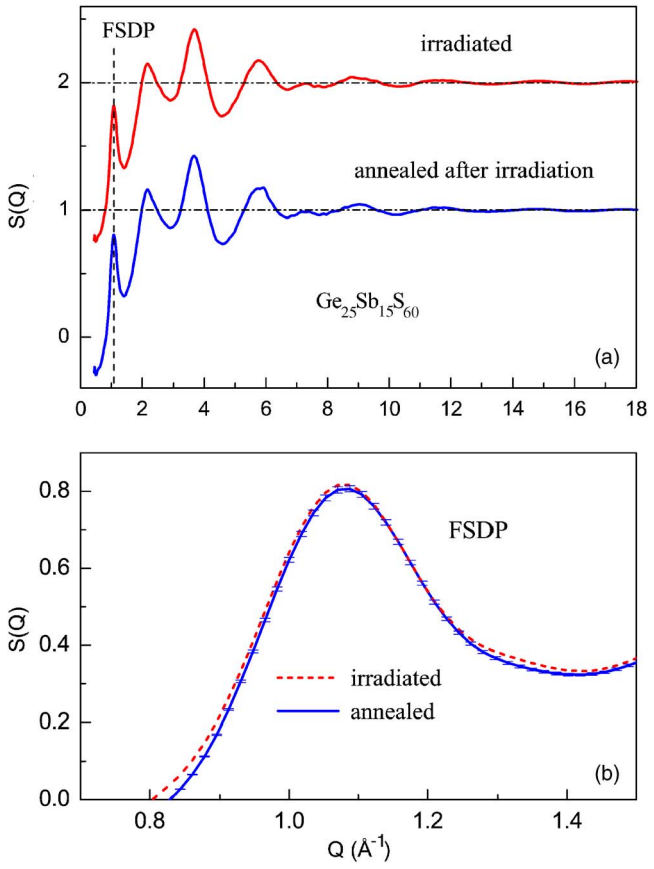

FIG. 1. (Color online) Experimental structure factors $S(Q)$ for $Ge_{25}Sb_{15}S_{60}$ glass in γ-irradiated [the curve for γ-irradiated state is shifted (+1) for clarity] and annealed after γ-irradiation states (a) and the FSDP γ-irradiated and annealed after γ-irradiation states (b). The change with irradiation at the FSDP maximum is comparable with the change at the tails of the FSDP.

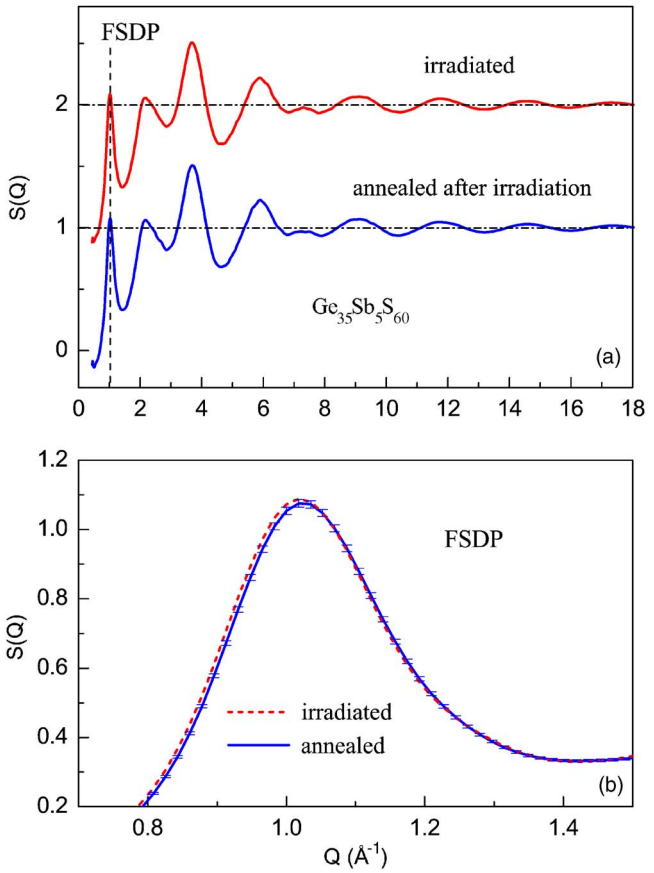

FIG. 2. (Color online) Experimental structure factors $S(Q)$ for $Ge_{35}Sb_5S_{60}$ glass in γ-irradiated [the curve for γ-irradiated state is shifted (+1) for clarity] and annealed after γ-irradiation states (a) and FSDP γ-irradiated and annealed after γ-irradiation states (b). The change with irradiation at the FSDP maximum is larger than the change at the tails of the FSDP.

as described in Ref. 12. As-prepared glasses were cut to the disklike specimens and polished to a high optical quality. Then, in order to remove possible mechanical strains formed after synthesis, the samples were annealed at about 10–20 K below the glass transition temperature [T_g=591 K for $Ge_{25}Sb_{15}S_{60}$ (Ref. 13) and T_g=643 K for $Ge_{35}Sb_5S_{60}$ (Ref. 13)].

Radiation treatment of glasses was performed by γ-quanta with an accumulated dose of 7.72 MGy at normal conditions of stationary radiation field created in a closed cylindrical cavity by a number of concentrically established ^{60}Co radioisotope capsules. No special measures were taken to prevent uncontrolled thermal annealing of the samples, but maximum temperature in the irradiating camera did not exceed 320–330 K during prolonged γ-irradiation (more than 30 days), providing absorbed dose power $P<5$ Gy/s. γ-irradiated samples were annealed at the same conditions as as-prepared glasses.

High-energy XRD experiments were carried out at the synchrotron experimental station BW5 at HASYLAB, DESY in Hamburg, Germany. All samples were examined in transmission geometry. The energy of radiation was 98.9 keV. Scattered intensity was measured between 0.5 and 18 Å^{-1}. Raw data were corrected for detector dead time, polarization, absorption, and variation in detector solid angle.[14] The scattering intensity measured in arbitrary units was converted into the coherent scattering intensity per atom in electronic units using the Krogh–Moe–Norman method.[15,16] Compton scattering was corrected using the values given by Cromer and Mann.[17] The Faber–Ziman[18] total structure factor $S(Q)$ was calculated from the scattering intensity as

$$S(Q) = \frac{I_{\text{e.u.}}^{\text{coh}}(Q) - \{\langle f^2(Q)\rangle - \langle f(Q)\rangle^2\}}{\langle f(Q)\rangle^2}, \quad (1)$$

with

$$\langle f^2(Q)\rangle = \sum_i c_i f_i^2(Q), \quad \langle f(Q)\rangle = \sum_i c_i f_i(Q), \quad (2)$$

where c_i is the molar fraction and $f_i(Q)$ is the total atomic scattering factor of the ith component of the glass.

The total pair distribution function $g(r)$ was obtained via transformation

$$g(r) = \frac{\rho(r)}{\rho_0} = 1 + \frac{1}{2\pi^2 r\rho_0}\int_0^\infty Q[S(Q)-1]\sin(Qr)dQ, \quad (3)$$

where $\rho(r)$ and ρ_0 are the local and the average number densities, respectively.

It is known that the impact on the experimental structure factors of chalcogenide glasses induced by γ-irradiation, hydrostatic pressure, or illumination are rather small.[9,19] Therefore, the experimental error should be minimized for correct

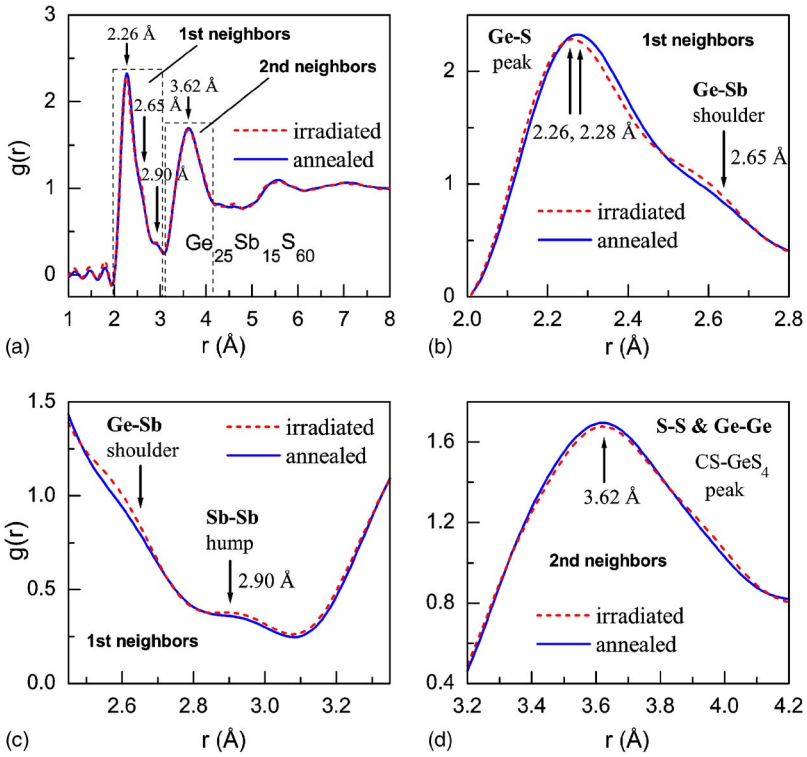

FIG. 3. (Color online) Parts of the pair distribution functions for $Ge_{25}Sb_{15}S_{60}$ glass in γ-irradiated and annealed after γ-irradiation states (see text for explanations).

investigation of such phenomena. In the present study, all XRD experiments were carried out within a couple of hours. The specimens were of the same thickness. They were fixed in a holder moving horizontally, which provided practically identical sample adjustment during measurements. All these helped to reduce the random error as much as possible.

III. RESULTS

Experimental structure factors $S(Q)$ for $Ge_{25}Sb_{15}S_{60}$ and $Ge_{35}Sb_5S_{60}$ glasses in γ-irradiated and annealed after γ-irradiation states are shown in Figs. 1 and 2. Oscillations in $S(Q)$ persist up to the high Q values for both samples; however they are more pronounced for the alloy with 35 at. % of Ge. The oscillations are symmetrical around unity, which is an evidence of proper experiments as well as correct normalization of the experimental intensities. The first sharp diffraction peak (FSDP) exists on the $S(Q)$ for both alloys studied. Intensity of the FSDP increases from $\sim$0.8 to $\sim$1.1 and its position shifts from 1.08 to 1.02 $Å^{-1}$ with increasing Ge content from 25 to 35 at. %. These findings agree with recently reported results for as-prepared $Ge_xSb_{40-x}S_{60}$ glasses.[10]

For both $Ge_{25}Sb_{15}S_{60}$ and $Ge_{35}Sb_5S_{60}$ compositions, position of maxima and minima on the structure factors of γ-irradiated and annealed glasses (including the FSDP) is practically the same [Figs. 1(a) and 2(a)]. Main differences between γ-irradiated and annealed glasses are observed in the intensity of the FSDP [Figs. 1(b) and 2(b)]. These differences are notably larger than the total experimental error of the structure factor, which is estimated to be below 1% at this range of Q. In the case of g-$Ge_{25}Sb_{15}S_{60}$, the change at the FSDP maximum is comparable with the change at the tails of the FSDP, while for g-$Ge_{35}Sb_5S_{60}$ the change at the FSDP maximum is larger than the change at the tails of the peak. At the same time, in the low-Q part of the peak, the FSDP becomes more asymmetrical with irradiation for composition with lower Ge content. The changes in the FSDP amplitude produced by high-energy γ-quanta in the present work are comparable with such effects observed for g-As_2S_3 under γ-irradiation[9] and hydrostatic pressure and illumination.[19] The effects on the prepeak can be enhanced in the case of neutron irradiation.[20]

Pair distribution function $g(r)$ obtained by the Fourier transformation of a structure factor $S(Q)$ is subjected to experimental errors.[21] This should be taken into account especially when small effects on $g(r)$ are considered like those in our study. Kaplow *et al.*[21] analyzed the effect of various errors on the pair distribution function and showed that they are manifested as false oscillations at different ranges of $g(r)$ (see Fig. 3 in Ref. 21). An error related to the improper normalization of the experimental intensity causes a very large peak close to r=0. Also an error in scattering factors is manifested at low r-values. An error due to the termination of the experimental data at a final value of the diffraction vector has a maximum in the vicinity of the first peak. Thus, the accuracy of the experimental data and data treatment could be judged from the analysis of the false oscillations appearing on the pair distribution function.

Figures 3 and 4 show the pair distribution functions $g(r)$ for $Ge_{25}Sb_{15}S_{60}$ and $Ge_{35}Sb_5S_{60}$ glasses, both in the γ-irradiated and annealed after γ-irradiation states. Small and symmetrical spurious oscillations on $g(r)$'s at r below the first maximum are indicative of small errors in normalization and scattering factors. Also, the termination error is not large due to high values of the diffraction vector accessed experimentally with short wave synchrotron radiation. This suggests that the differences on the pair distribution func-

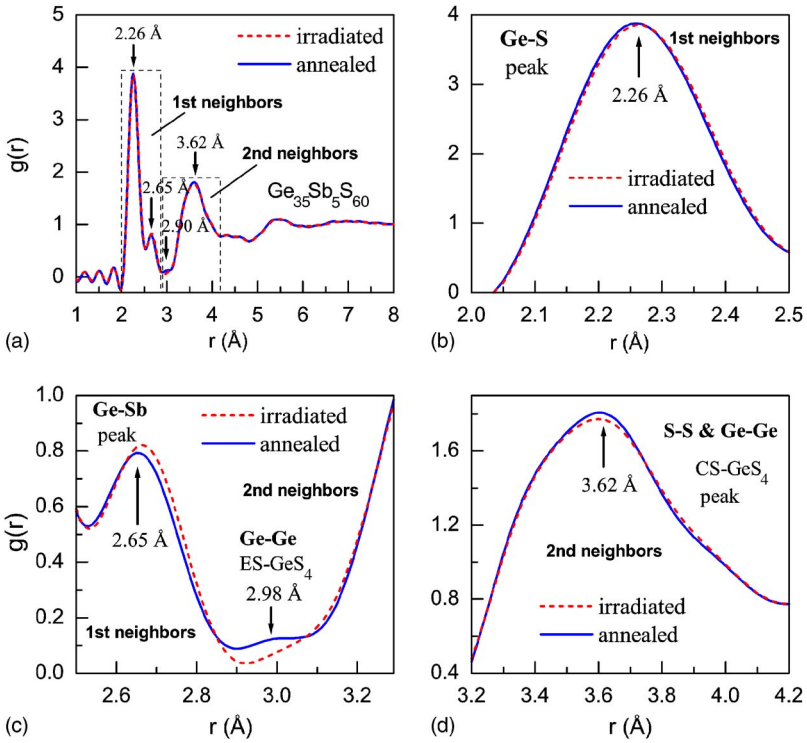

FIG. 4. (Color online) Parts of the pair distribution functions for $Ge_{35}Sb_5S_{60}$ glass in γ-irradiated and annealed after γ-irradiation states (see text for explanations).

tions observed can be related to the structural changes in $Ge_{25}Sb_{15}S_{60}$ and $Ge_{35}Sb_5S_{60}$ glasses due to irradiation/annealing.

For the $Ge_{25}Sb_{15}S_{60}$ glass, the following features that can be attributed to the nearest neighbor correlations are found: a peak at $r=2.26$ Å, a shoulder at $r\approx2.65$ Å, and a hump at $r\approx2.90$ Å. The maximum at $r=3.62$ Å reflects the second coordination sphere. For $Ge_{35}Sb_5S_{60}$ glass, two peaks (at 2.26 and 2.65 Å) are resolved in the first coordination shell, and a peak at 3.62 Å belonging to the second coordination shell is seen. Also a hump at $r\approx2.98$ Å is observed on $g(r)$ of $Ge_{35}Sb_5S_{60}$ glass. The intensity of peaks at 2.26 and 3.62 Å remarkably increases and a well-resolved peak at 2.65 Å appears on the pair distribution function when Ge amount changes from 25 to 35 at. %. The results obtained are summarized in Table I.

Annealing of γ-irradiated samples results in increasing intensity of the peak at 2.26 Å (effect being larger for $Ge_{25}Sb_{15}S_{60}$ with shift of the peak position to a higher Q value) and decreasing intensity of the peaks at 2.65, 2.90, and 3.62 Å. It is interesting that the hump at 2.98 Å is found only for $Ge_{35}Sb_5S_{60}$ in the annealed state and it is practically invisible in the γ-irradiated state.

IV. DISCUSSION

As it has already been mentioned, Kakinuma *et al.*[10] studied the structure of $Ge_xSb_{40-x}S_{60}$ ($x=10$, 20, and 30) glasses with neutron diffraction. They found three peaks in the pair distribution functions at 2.24 ± 0.02, 2.48 ± 0.02, and 3.61 ± 0.03 Å. The peaks at 2.24 and 3.61 Å detected for all compositions were attributed to Ge–S correlations in the first coordination shell and to Ge–Ge, Ge–Sb, and Sb–Sb correlations in the second coordination shell, respectively. The

TABLE I. Structural parameters of $Ge_{25}Sb_{15}S_{60}$ and $Ge_{35}Sb_5S_{60}$ glasses γ-irradiated (irrad.) and annealed after γ-irradiation (ann.) states. r_i, position, and $g(r_i)$, intensity of peaks (shoulders, humps) on the pair distribution functions. The errors are estimated from the Gaussian fits of the peaks.

Glasses	State	r_1(Å) ± 0.01	$g(r_1)$	r_2(Å) ± 0.01	$g(r_2)$	r_3(Å) ± 0.02	$g(r_3)$
First coordination shell (first-nearest-neighbor correlations)							
$Ge_{25}Sb_{15}S_{60}$	irrad.	2.26	2.28	shoulder	···	2.90 (hump)	0.38
	ann.	2.28	2.33	shoulder	···	2.90 (hump)	0.35
$Ge_{35}Sb_5S_{60}$	irrad.	2.26	3.86	2.66	0.82	···	···
	ann.	2.26	3.88	2.65	0.79	···	···

Glasses	State	r_4(Å) ± 0.02	$g(r_4)$	r_5(Å) ± 0.01	$g(r_5)$
Second coordination shell (second-nearest-neighbor correlations)					
$Ge_{25}Sb_{15}S_{60}$	irrad.	···	···	3.62	1.68
	ann.	···	···	3.62	1.70
$Ge_{35}Sb_5S_{60}$	irrad.	···	···	3.60	1.77
	ann.	2.98 (hump)	0.12	3.60	1.81

peak at 2.48 Å was clearly resolved only for $Ge_{10}Sb_{30}S_{60}$ glass and it was related to the first neighbor contribution Sb–S.

In agreement with Ref. 10, the first peak on $g(r)$ at 2.26 ± 0.01 Å for $Ge_{25}Sb_{15}S_{60}$ and $Ge_{35}Sb_5S_{60}$ glasses studied in the present work can also be attributed to the Ge–S correlations. This value (2.26 Å) is also consistent with 2.21–2.24 Å distances corresponding to Ge–S first neighbors in $GeS_{4/2}$ tetrahedra for germanium sulfide glasses.[22]

Kakinuma *et al.*[10] observed a peak at 2.48 ± 0.02 Å on the $g(r)$ for $Ge_{10}Sb_{30}S_{60}$, which transformed into a shoulder for the alloys with 20 and 30 at. % of Ge. They attributed this peak (shoulder) to Sb–S correlations. We also see a shoulder on the pair distribution function for $Ge_{25}Sb_{15}S_{60}$ and a distinct peak for $Ge_{35}Sb_5S_{60}$ glass, however at somewhat higher r-value: at 2.65 ± 0.01 Å. This value is comparable to Ge–Sb bond length (~2.7 Å) detected by extended x-ray absorption fine structure (EXAFS) (Ref. 23) as well as to the sum of covalent radii of Ge and Sb atoms [2.6 Å (Ref. 22), 2.67 (Ref. 24)]. It is clear that Sb–S contributions to the total $g(r)$ dominate in the $Ge_xSb_{40-x}S_{60}$ glasses with high Sb content, whereas contribution from Ge–Sb correlations increases as the Ge content becomes larger. This experimental finding regarding Ge–Sb correlations agrees well with bond statistics within random bond network model[25,26] and actually with Feltz's[12] suggestion about the existence of As_2Ge structural units and/or Ge–As bonds in $Ge_xAs_{40-x}S_{60}$ ternaries for compositions with $x > 30$. This means that in the alloys studied, random bonding is dominant in comparison with the ordered bond network model[25,26] in the framework of which the weakest bonds such as Ge–Sb(As) in Ge–Sb(As)–S systems do not contribute to the bond fractions.

Ge–Ge (2.38–2.52 Å) (Ref. 22) and S–S (2.05–2.06 Å) (Ref. 22) first neighbor correlations (if exist) cannot be resolved on the pair distribution functions. They can simply be covered by the peak from Ge–S contributions. Moreover, we suppose that S–S bonds are very improbable in the glass matrix because $Ge_{25}Sb_{15}S_{60}$ and $Ge_{35}Sb_5S_{60}$ alloys are nonstoichiometric with an overstoichiometry of metal atoms (Ge, Sb).

A hump on the pair distribution functions observed at ~2.90 Å for $Ge_{25}Sb_{15}S_{60}$ and at ~2.98 Å for $Ge_{35}Sb_5S_{60}$ glass might be caused by the termination effect. It is, however, interesting that the value of 2.90 Å well correlates with Sb–Sb bond length.[24] Taking into account changes in the intensity on $g(r)$ at ~2.90 Å under irradiation/annealing treatment and practical disappearance of this hump for $Ge_{35}Sb_5S_{60}$ glass, we may suppose that this (hump) can be related to the Sb–Sb contributions. Also, the hump around 3.0 Å in the total pair distribution function of GeX_2-based glasses is known to result from the short Ge–Ge second neighbor correlations in the edge-shared (ES) tetrahedra.[27] This means that the hump on the $g(r)$ for $Ge_{35}Sb_5S_{60}$ glass at ~2.98 Å may reflect atomic contributions of Ge–Ge second neighbors in ES-GeS_4. It should be noted that ES configurations in the tetrahedral-type glasses are also intensively studied by Raman spectroscopy and *ab initio* calculations.[28,29]

It is difficult to resolve the peak located at 3.62 Å on the pair distribution functions for both alloys studied. Kakinuma *et al.*[10] attributed this peak to the secondary partial correlations Ge–Ge, Ge–Sb, Sb–Sb, and S–S. In principle, all these correlations may exist. We also observe that the intensity of this peak increases and its position shifts to lower Q-values with increasing Ge concentration (see Table I). Besides, ratio of peak positions at 3.62 and 2.26–2.28 Å for the glasses studied is 1.59–1.60. This is somewhat smaller than the value of $\sqrt{8/3} = 1.63$ for perfect tetrahedra, which can be a result of $GeS_{4/2}$ unit deformation (probably by increasing concentration in Ge–Ge bonding[30]). It should also be noted here that the structural study of germanium sulfide glasses[22] shows that the broad peak at ~3.6 Å corresponds to S–S second neighbors and longer Ge–Ge correlations in corner-shared $GeS_{4/2}$ tetrahedra (CS-GeS_4).

Let us consider the radiation-/annealing-induced structural changes in $Ge_{25}Sb_{15}S_{60}$ and $Ge_{35}Sb_5S_{60}$ glasses. If the main peak on $g(r)$ at 2.26 Å is related to Ge–S first neighbor correlations, then variation in its intensity can be explained by radiation-induced structural transformations in $GeS_{4/2}$ tetrahedra. According to the optical observations,[8,30] the radiation-induced optical effect (RIOE) is absent in Sb-rich $Ge_xSb_{40-x}S_{60}$ glasses. However it appears and increases with increasing Ge concentration. It is interesting that RIOE reaches a maximum in magnitude for $x = 27$. Therefore, it was concluded[30] that the radiation-induced structural changes in $Ge_xSb_{40-x}S_{60}$ glasses are mainly connected with the Ge–S subsystem, while Sb atoms play a role for annihilation of radiation-induced defects.

The average coordination number in $Ge_{25}Sb_{15}S_{60}$ glass calculated as the number of covalent chemical bonds per atom of the formula unit equals 2.65. This value is close to a characteristic parameter of topological phase transition from a two-dimensional layerlike structure to a three-dimensional cross-linked structural network in chalcogenide glasses ($Z = 2.67$) suggested by Tanaka.[31] Thus, the anomalous compositional behavior of RIOE (Refs. 8 and 30) and its extremum at 27 at. % Ge can be related to the topological changes in $Ge_xSb_{40-x}S_{60}$ glasses ($Z = 2.67$ for $Ge_{27}Sb_{13}S_{60}$). This can also explain (i) why the radiation-/annealing-induced changes in the intensity of the main peak at 2.26 Å (Ge–S correlations) are larger for g-$Ge_{25}Sb_{15}S_{60}$ as compared to g-$Ge_{35}Sb_5S_{60}$, and (ii) why the change in the first peak position is observed only for $Ge_{25}Sb_{15}S_{60}$ composition [Figs. 3(b) and 4(b), Table I].

Structural changes in Ge–S subsystem upon γ-irradiation can be related to breaking Ge–S covalent chemical bonds and their switching into S–S bonds with the appearance of under- and overcoordinated coordination topological defects (CTDs)[32] Ge_3^- and S_3^+ (Fig. 5). Such transformations explain the reduction in intensity of the peaks at 2.26 Å (Ge–S first neighbor correlations) and at 3.62 Å (S–S and Ge–Ge second neighbor correlations in CS-GeS_4 tetrahedra) for γ-irradiated samples in comparison with annealed glasses [Figs. 3(b), 3(d), 4(b), and 4(d)]. Creation of defective pairs (Ge_3^-,S_3^+) in glass matrix is accompanied by the formation of additional free volume in the vicinity of negatively charged CTD due to the redistribution of the electronic density in the framework of bond-free solid angle (BFSA) concept suggested by Kastner[33] (Fig. 5). This is important for

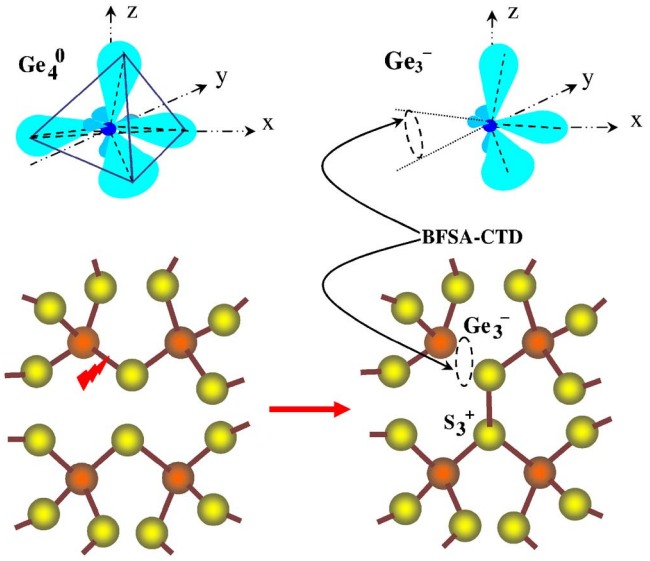

FIG. 5. (Color online) Radiation-induced formation of CTDs Ge_3^- and S_3^+ in Ge–S based subsystem (Ref. 32) and appearance of additional free volume in the vicinity of negatively charged CTD in the framework of BFSA concept (Ref. 33) (see text for details).

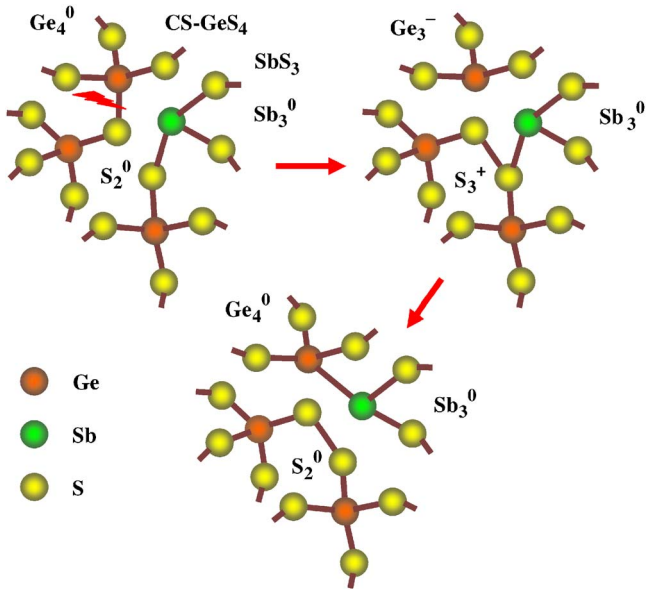

FIG. 6. (Color online) Formation of Ge–Sb bonds with normal atomic coordination in their vicinity (Ge_4^0, Sb_3^0, S_2^0) as a result of radiation-induced structural transformations in corner-shared GeS_4 tetrahedra (CS-GeS_4) with intermediate structural configuration accompanied by the appearance of unstable CTDs Ge_3^- and S_3^+ (see text for details).

understanding radiation-/annealing-induced changes in the FSDP on the structure factors of $Ge_{25}Sb_{15}S_{60}$ and $Ge_{35}Sb_5S_{60}$ glasses [Figs. 1(b) and 2(b)]. We suppose that increasing intensity of the FSDP with increasing Ge content could be explained (i) with the so-called "void-based model" introduced in first principles by Wright *et al.*[34] and developed later by Elliott,[35] and (ii) within the approach of Bychkov *et al.*[36] based on the network-forming cation (NFC) related structural units.

In the void-based model, the FSDP is associated with the periodicity arising from the boundaries between a succession of the cages that comprise the structure (Wright *et al.*[34]) and/or chemical ordering of interstitial voids (i.e., the centers of the cages) around cation-centered clusters in the structure (Elliott[35]). Ordering of interstitial voids around Ge boundaries might be supposed to increase in the $Ge_xSb_{40-x}S_{60}$ glasses with increasing Ge content. This should result in rising FSDP within the void-based model.

The void-based model is well applicable for the interpretation of the FSDP origin not only in chalcogenide and oxide glasses[37–40] but also in other amorphous solids, for instance, low-density amorphous water.[41] However, it should be noted that this concept alone cannot always explain the origin of the FSDP.[42,43] In such situation, the approach of Bychkov *et al.*[36] based on the NFC structural units, which relates FSDP with multiple changes in the glass network both on the short- and medium-range scales, comes under consideration.

We suppose that the changes observed on the short-range (first and second neighbor correlations) and intermediate-range distances in $Ge_{25}Sb_{15}S_{60}$ and $Ge_{35}Sb_5S_{60}$ glasses are interconnected. Formation of Ge_3^- CTDs and appearance of additional free volume lead to increasing concentration of voids (or their volume) around Ge-centered clusters. However, less fraction of homopolar and heteropolar NFC-NFC correlations for g-$Ge_{25}Sb_{15}S_{60}$ in comparison with g-$Ge_{35}Sb_5S_{60}$ does not affect the FSDP amplitude [Figs. 1(b) and 3(b)] [even if the structural changes in the vicinity of the main peak at 2.26 Å (Ge–S first neighbor correlations) are more pronounced for $Ge_{25}Sb_{15}S_{60}$ composition]. At the same time, increasing the FSDP intensity upon irradiation for the glass with higher Ge content ($Ge_{35}Sb_5S_{60}$) can be explained by both effects: increasing concentration of voids (or voids' volume) around Ge-centered clusters (formation of Ge_3^- CTDs) and increasing fraction of heteropolar NFC-NFC (Ge–Sb) first neighbor correlations [Figs. 2(a), 4(b), and 4(c)]. This means that the void model alone is not enough for the explanation of the FSDP changes observed, as pointed out also in Ref. 43. Our results demonstrate that combination of the void model[34,35] and NFC-related structural units[36] is quite applicable to interpret the radiation-/annealing-induced changes in the FSDP intensity and confirm a relation of the FSDP both with short- and intermediate-range scales.

Higher peak intensity at 2.65 Å (Ge–Sb first neighbor correlations) on the pair distribution function for g-$Ge_{35}Sb_5S_{60}$ upon γ-irradiation as compared to the annealed sample (Fig. 4) can be explained by a mechanism schematically shown in Fig. 6. Considering that the corner-sharing tetrahedral (CS-GeS_4) bonding is dominant in the Ge-rich $Ge_xSb_{40-x}S_{60}$ glasses, and bearing in mind results of the Raman spectroscopy,[44] we suppose that the main structural configurations involved in the mechanism of radiation-induced structural transformations (Fig. 6) are CS-GeS_4 tetrahedra and tetrahedral $GeS_{4/2}$ (or GeS_4, for simplicity) and pyramidal $SbS_{3/2}$ (or SbS_3) units linked through Ge–S–Sb bridge. γ-Irradiation of $Ge_xSb_{40-x}S_{60}$ glasses results in breaking Ge–S bonds in CS-GeS_4 tetrahedra with the next switching into S–S bonds, which leads to the appearance of Ge_3^- and S_3^+ CTDs. However, due to the existence of heavy Sb atoms with high metallization ability in the vicinity of defective pairs (Ge_3^-,S_3^+), they (pairs) are unstable in contrast to those

that are stable in the structural configuration without Sb (Fig. 5). Finally, new Ge–Sb bonds with normal fourfold and threefold coordinations of Ge and Sb atoms, respectively, and S–S dimers with normal twofold coordination of S atoms are created after irradiation. We suppose that γ-irradiation-induced changes in intensity of peaks on $g(r)$ for $Ge_{35}Sb_5S_{60}$ glass at 2.65 and 3.62 Å [opposite upon annealing; see Figs. 4(c) and 4(d)] are related to the formation of new Ge–Sb correlations, which in due course are related to the transformations of Ge–S first neighbors (peak at 2.26 Å) and S–S/Ge–Ge second neighbors in CS-GeS_4 (peak at 3.62 Å). Also, this shows that the changes in the first and second coordination shells within two mechanisms [radiation-induced structural transformations in the CS-GeS_4 configuration with defects, i.e., formation of (Ge_3^-, S_3^+) CTDs, and without defects, i.e., formation of Ge–Sb bonds with normal atomic coordination] are interconnected, which are consistent with the behavior of the FSDP mentioned earlier. The fact that the peak at 2.65 Å does not completely disappear upon annealing indicates that Ge–Sb correlations in the first coordination shell also exist in the glass matrix in the initial (unexposed) state. This seems to be an evidence for the existence of Sb_2Ge structural units and/or Ge–Sb bonds in as-prepared $Ge_xSb_{40-x}S_{60}$ glasses for compositions with $x>30$ similar to the assumption of Feltz for the $Ge_xAs_{40-x}S_{60}$ system.[12] This result correlates with EXAFS data for glass compositions in stoichiometric $(Sb_2S_3)_x(GeS_2)_{1-x}$ system[23] and conclusions of Kakinuma *et al.*[10] for $Ge_xSb_{40-x}S_{60}$ glasses in nonstoichiometric $(Sb_2S_3)_x(Ge_2S_3)_{1-x}$ system.

A similar mechanism seems to be appropriate for the explanation of the radiation-/annealing-induced changes in the Sb–Sb bonds in the first coordination shell detected as a hump on $g(r)$ at 2.90 Å [Fig. 3(c)]. It is noticeable that such transformations take place for $Ge_{25}Sb_{15}S_{60}$ but not for $Ge_{35}Sb_5S_{60}$ where the amount of Sb is smaller. Schematic illustration of increasing in Sb–Sb bonding in the γ-irradiated state of the sample is shown in Fig. 7. In this scheme, the under- and overcoordinated Sb_2^- and S_3^+ CTDs created after irradiation are unstable due to the Sb ability for annihilation of charged defects in its vicinity. As a result, defects with wrong atomic coordinations Sb_2^- and S_3^+ are transformed to the normally coordinated atoms Sb_3^0 and S_2^0, and, finally, new nondefective Sb–Sb bonds are formed. For more detailed information in this connection, the EXAFS measurements are needed.

Also, we would like to mention the hump on $g(r)$ for $Ge_{35}Sb_5S_{60}$ glass at 2.98 Å, which might be related to Ge–Ge second neighbor correlations in ES-GeS_4 tetrahedra [Fig. 4(c)]. We suppose that the appearance of this hump (2.98 Å) after annealing of γ-irradiated $Ge_{35}Sb_5S_{60}$ glass can be explained by a mechanism presented in Fig. 8. Switching of Ge–S into S–S bonds in the case of edge-sharing tetrahedral bonding (ES-GeS_4) results in the disappearance of ES-GeS_4 configuration due to the formation of Ge_3^- and S_3^+ CTDs, where S_3^+ defect is created in the form of S–S cluster edge dimmers intensively reported in the experimental and theoretical data by using Raman spectroscopy and *ab initio* calculations.[28,29] Appearance of the hump at 2.98 Å upon annealing seems to be additional evidences for this mechanism.

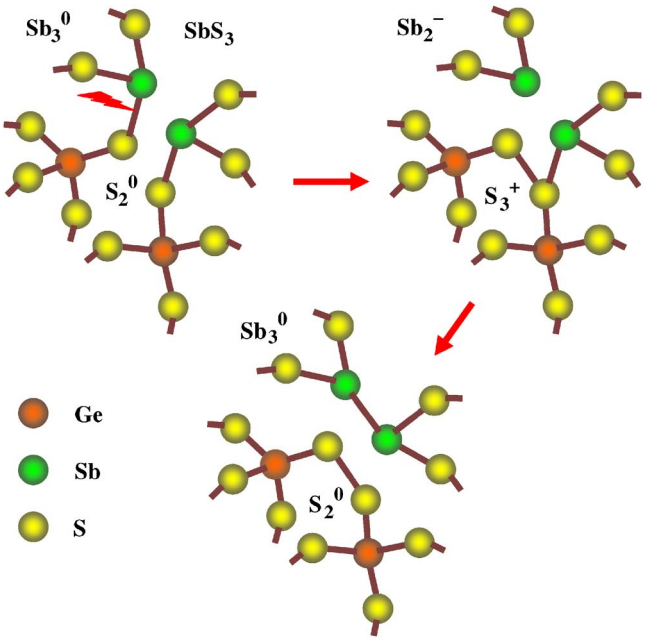

FIG. 7. (Color online) Formation of Sb–Sb bonds with normal atomic coordination in their vicinity (Sb_3^0, S_2^0) as a result of radiation-induced structural transformations in SbS_3 pyramids with intermediate structural configuration accompanied by the appearance of unstable CTDs Sb_2^- and S_3^+ (see text for details).

V. SUMMARY

Impact of γ-irradiation and subsequent annealing on the atomic structure of $Ge_{25}Sb_{15}S_{60}$ and $Ge_{35}Sb_5S_{60}$ glasses has been studied with high-energy synchrotron XRD. Analysis of the experimental structure factors and pair distribution functions revealed the differences related to the structural changes at the short- and intermediate-range scales in the glasses studied.

Radiation-/annealing-induced changes in $Ge_xSb_{40-x}S_{60}$ glasses can be described by a combination of at least three various mechanisms in the framework of CTD and BFSA concepts: first mechanism—radiation-induced structural transformations in the CS-GeS_4 configuration with defects, i.e., formation of (Ge_3^-, S_3^+) CTDs (Fig. 5); second mechanism—radiation-induced structural transformations in the CS-GeS_4 tetrahedral and SbS_3 pyramidal configurations without defects, i.e., formation of Ge–Sb and Sb–Sb bonds with normal atomic coordination (Figs. 6 and 7); third

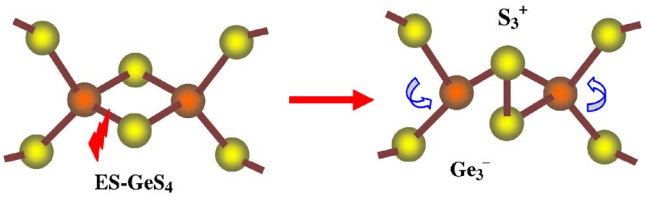

FIG. 8. (Color online) Radiation-induced formation of CTDs Ge_3^- and S_3^+ in the case of edge-shared GeS_4 tetrahedra (ES-GeS_4).

mechanism—radiation-induced structural transformations in the ES-GeS_4 configuration with defects, i.e., formation of (Ge_3^-,S_3^+) CTDs (Fig. 8).

Origin of the FSDP on the structure factors of $Ge_{25}Sb_{15}S_{60}$ and $Ge_{35}Sb_5S_{60}$ glasses is explained in terms of the void-based model[34,35] and network-forming cation-cation structural units.[36] It is established that the combination of these approaches can interpret plausibly the radiation-/annealing-induced changes in the FSDP intensity.

ACKNOWLEDGMENTS

The authors would like to thank Dr. P. Jovari (Research Institute for Solid State Physics and Optics, Budapest, Hungary) for his help with experimental data treatment. T.K. gratefully acknowledges INTAS for Young Scientist Fellowship (Ref. No. 05-109-5323) and his stay in Chemnitz University of Technology (Germany) and Jan Dlugosz University in Czestochowa (Poland). T.K. and I.K. also acknowledge Deutsches Elektronen-Synchrotron DESY for support of the experiments performed at HASYLAB (Hamburg, Germany).

[1] I. V. Kityk and B. Sahraoui, J. Chem. Phys. **14**, 8105 (2001).
[2] A. Saliminia, A. Villeneuve, T. V. Galstyan, S. La Rochelle, and K. Richardson, J. Lightwave Technol. **17**, 837 (1999).
[3] G.-F. Zhou, Mater. Sci. Eng., A **304-306**, 73 (2001).
[4] T. Ohta, M. Birukawa, N. Yamada, and K. Hirao, J. Magn. Magn. Mater. **242-245**, 108 (2002).
[5] A. V. Kolobov, P. Fons, A. I. Frenkel, A. L. Ankudinov, J. Tominaga, and T. Uruga, Nature (London) **3**, 703 (2004).
[6] C. Zha, R. Wang, A. Smith, A. Prasad, R. A. Jarvis, and B. L. Davies, J. Mater. Sci.: Mater. Electron. **18**, S389 (2007).
[7] A. Srinivasan, K. N. Madhusoodanan, E. S. R. Gopal, and J. Philip, Phys. Rev. B **45**, 8112 (1992).
[8] O. I. Shpotyuk, R. Ya. Golovchak, T. S. Kavetskyy, A. P. Kovalskiy, and M. M. Vakiv, Nucl. Instrum. Methods Phys. Res. B **166**&167, 517 (2000).
[9] T. Kavetskyy, O. Shpotyuk, I. Kaban, and W. Hoyer, J. Optoelectron. Adv. Mater. **9**, 3247 (2007).
[10] F. Kakinuma, T. Fukunaga, and K. Suzuki, J. Non-Cryst. Solids **353**, 3045 (2007).
[11] O. I. Shpotyuk, A. P. Kovalskiy, T. S. Kavetskyy, and R. Ya. Golovchak, J. Non-Cryst. Solids **351**, 993 (2005).
[12] A. Feltz, *Amorphous and Vitreous Inorganic Solids* (Mir, Moscow, 1986).
[13] V. Pamukchieva, E. Savova, and M. Baeva, Phys. Chem. Glasses **36**, 328 (1998).
[14] H. F. Poulsen, J. Neuefeind, H.-B. Neumann, J. R. Schneider, and M. D. Zeidler, J. Non-Cryst. Solids **188**, 63 (1995).
[15] J. Krogh-Moe, Acta Crystallogr. **9**, 951 (1956).
[16] N. Norman, Acta Crystallogr. **10**, 370 (1957).
[17] D. T. Cromer and J. B. Mann, J. Chem. Phys. **47**, 1892 (1967).
[18] T. E. Faber and J. M. Ziman, Philos. Mag. **11**, 153 (1965).
[19] H. Hamanaka, S. Minomura, and K. Tsuji, J. Non-Cryst. Solids **137**&138, 977 (1991).
[20] A. C. Wright, B. Bachra, T. M. Brunier, R. N. Sinclair, L. F. Gladden, and R. L. Portsmouth, J. Non-Cryst. Solids **150**, 69 (1992).
[21] R. Kaplow, S. L. Strong, and R. L. Averbach, Phys. Rev. **A138**, 1336 (1965).
[22] E. Bychkov, M. Miloshova, D. L. Price, C. J. Benmore, and A. Lorriaux, J. Non-Cryst. Solids **352**, 63 (2006).
[23] L. Cervinka, O. Smotlacha, J. Bergerova, and L. Tichy, J. Non-Cryst. Solids **137**&138, 123 (1991).
[24] http://www.webelements.com/
[25] E. Vateva, E. Skordeva, and D. Arsova, Philos. Mag. B **67**, 225 (1993).
[26] D. Arsova, J. Phys. Chem. Solids **57**, 1279 (1996).
[27] N. Ramesh Rao, P. S. R. Krishna, S. Basu, B. A. Dasannacharya, K. S. Sangunni, and E. S. R. Gopal, J. Non-Cryst. Solids **240**, 221 (1998).
[28] P. Boolchand, J. Grothaus, M. Tenhover, M. A. Hazle, and R. K. Grasselli, Phys. Rev. B **33**, 5421 (1986).
[29] N. Mateleshko, V. Mitsa, and R. Holomb, Physica B **349**, 30 (2004).
[30] A. Kovalskiy, T. Kavetskyy, J. Plewa, and O. Shpotyuk, Solid State Phenom. **90–91**, 241 (2003).
[31] Ke. Tanaka, Phys. Rev. B **39**, 1270 (1989).
[32] R. Ya. Golovchak and O. I. Shpotyuk, Philos. Mag. **85**, 2847 (2005).
[33] M. Kastner, Phys. Rev. B **7**, 5237 (1973).
[34] A. C. Wright, R. N. Sinclair, and A. J. Leadbetter, J. Non-Cryst. Solids **71**, 295 (1985).
[35] S. R. Elliott, Phys. Rev. Lett. **67**, 711 (1991).
[36] E. Bychkov, C. J. Benmore, and D. L. Price, Phys. Rev. B **72**, 172107 (2005).
[37] S. R. Elliott, Nature (London) **354**, 445 (1991).
[38] S. R. Elliott, J. Phys.: Condens. Matter **4**, 7661 (1992).
[39] A. C. Wright, J. Non-Cryst. Solids **179**, 84 (1994).
[40] M. Nakamura, M. Arai, Y. Inamura, T. Otomo, and S. M. Bennington, Phys. Rev. B **67**, 064204 (2003).
[41] S. R. Elliott, J. Chem. Phys. **103**, 2758 (1995).
[42] F. H. M. van Roon, C. Massobrio, E. de Wolff, and S. W. de Leeuw, J. Chem. Phys. **113**, 5425 (2000).
[43] C. Massobrio and A. Pasquarello, J. Chem. Phys. **114**, 7976 (2001).
[44] I. P. Kotsalas, D. Papadimitriou, C. Raptis, M. Vlcek, and M. Frumar, J. Non-Cryst. Solids **226**, 85 (1998).